Defence Science Journal, Vol. 73, No. 4, July 2023, pp. 457-467, DOI : 10.14429/dsj.73.18686

Experimental Investigation and Thermophysics Analysis of Joule-Thomson Cooler Applicable to Infrared Imaging

Mayank Singhal[#,*], Rajesh Kumar[$], R.S. Walia[!] and Sanjay Kumar Pandey[^]

[#]*Defence Research and Development Organisation, SSPL Complex, Timarpur, Delhi -110054, India*

[$]*Department of Mechanical Engineering, Delhi Technological University, Delhi - 110 042, India*

[!]*Department of Production and Industrial Engineering, Punjab Engineering College, Chandigarh - 160 012, India*

[^]*Defence Research and Development Organisation, Metcalfe House, Delhi - 110 054, India*

[*]*E-mail: mayanksinghal25@gmail.com*

ABSTRACT

Recuperative type of heat exchanger (H-E) based miniature Joule-Thomson (J-T) cooler operated in the steady-state condition is employed extensively in applications towards infrared detectors cooling, thermal imaging cameras, and homing guidance devices in a wide variety of defence projectile systems. In this study, a theoretical thermal design of recuperative H-E for determining a viable geometry using iterative methodology is discussed. A steady-state numerical analysis for the developed geometrical model of the H-E is also reported, along with the experimental studies for typical operating conditions. A custom numerical code using the Runge-Kutta method has been developed in MATLAB, and the results from the code compared with predictions of COMSOL multi-physics are in good agreement. Further, results have been validated proving the efficacy of the theoretical model and custom numerical code developed.

Keywords: JT cooler; Steady-state characteristics; Infrared radiation; Recuperative heat exchanger; Effectiveness

NOMENCLATURE

A : Cross-sectional area of flow passage (m^2)
C_p : Specific heat at constant pressure $\left(J/k_g - K\right)$
C : Heat capacity rate of fluids defined by the product of m and $C_P(W/K)$
C_r : Heat capacity ratio
d : Diameter (m)
d_{if} : Inner diameter of finned tube (m)
d_{of} : Outer diameter of finned tube (m)
d_{ofb} : Outer diameter of finned tube without fins(m)
D_h : Helix diameter (m)
f : Fanning friction factor
g_f : Gap between two fins (m)
G : Mass velocity, $\left(K_g/m^2 - s\right)(G = m/A)$
h : Coefficient of Heat Transfer $(W/m^2 - K)$
k : Thermal conductivity of wall material $(W/m - K)$
L : Length of heat exchanger (m)
$\dot{m}$: Mass flow rate $\left(k_g/s\right)$
N_f : Number of fins
N : Number of transfer units for individual fluid stream
NTU : Overall number of transfer units
P : Perimeter of heat transfer (m)
Q : Heat transfer (watt)
U : Overall heat transfer coefficient $(W/m^2 - K)$
x Axial co-ordinate of heat exchanger (m)
X : Dimensionless axial co-ordinate in heat exchanger defined by x/L

Greek symbols

σ : Stefan Boltzmann constant (W / m^2K^4)
ρ : Density of the working medium $\left(k_g/m^3\right)$
ε_s : Emissivity of the outer shield
ε_r : Emissivity of the ambient
ϕ : Dimensionless pressure
θ : Dimensionless temperature
η_o : Adiabatic efficiency
η_f : Efficiency of the fin
Γ : Relative residual flux

Subscripts

1-5 : State points
a : Ambient
c : Cold fluid
c_i : Capillary inside
c_o : Capillary outside
f : Fin
f_t : Fin tube
h : Hot fluid or high-pressure gas

Received : 23 November 2022, Revised : 09 March 2023
Accepted : 29 March 2023, Online published : 11 July 2023

in : Inlet
m : Mandrel
m_o : Mandrel outside
o : Outer
out : Outlet
r : Radiation
s : Shield
s_i : Shield inside
s_o : Shield outside
w : Wall of finned capillary

1. INTRODUCTION

All objects having surface temperatures more than absolute zero are found to be emitting thermal radiation, generated due to inherent vibration and rotation of atoms and molecules. Some part of this thermal radiation falls in the Infrared (IR) zone. Hence, the higher the temperature of an object, the greater is induced molecular motion leading to higher emitted infrared energy. InfraRed (IR) imaging primarily utilizes this property for various applications spanning diverse domains.

Hu[1], *et al.* developed a dual-camera imaging system having a far-infrared imager, an IR camera with an IR range cut lens, and a lighting array. The same was used for measuring breathing rate (BR) and heart rate (HR) simultaneously without much effort and attention during nighttime. Vollmer and Mollman[2] in addition to discussing advanced methods of Infrared imaging have also dwelled in detail on the detection of gases using infrared imaging. Bhan and Dhar[3] discussed the fundamentals of Infrared detectors, the latest trends, and new applications in the area of Infrared imaging.

Although in recent times Infrared imaging finds several civil and industrial applications owing to its better economic viability, it continues to be an area of focus in defense research due to its great significance in surveillance and target detection in the dark. Contemporary research in the area of InfraRed imaging and technology includes the fabrication of sensors involving the use of novel materials, reduced pixel pitch (basically the distance between two-pixel centers), and state-of-the-art technologies for detector cooling and vacuum integrity.

Cooling technology is a critical subset of IR imaging technology as IR detectors function at their optimal only at cryogenic temperatures. In this context, Joule-Thomson (J-T) coolers of miniature type are utilised for sub-zero cooling in applications such as superconducting electronics, low noise amplifiers, optical detectors in space applications, and for maintaining temperatures of various IR sensors (i.e., IR sensitive elements) within desired limits.

This miniature J-T cryocooler, when operated in a steady-state condition, is extensively employed for fast cooling of IR detectors, night vision cameras, homing heads, and guidance systems of missiles. J-T cooler finds applications mainly due to the benefit of its configuration being simple and compact with a rapid cooling capability[4-5]. Joule –Thomson (J-T) effect is defined as cooling power that is generated when a gas with high pressure flows through a throttling device undergoing isenthalpic expansion. Several numerical and experimental studies involving the cooling performance, heat exchanger, and clogging dynamics of the miniature J-T cooler have been carried out.

Xue[6], *et al.* have generated a model of the counter-flow heat exchanger of the Hampson type. The theoretical model developed is used for analysing the performance of the miniature J-T cooler having a recuperative kind of heat exchanger. It reported that effectiveness decreases with increasing inlet pressure, although the overall effectiveness still exceeds 95 %. Ng[7], *et al.* tracked the thermal and fluid properties of Argon expanding in the cooler utilizing a model based on a fully distributed simulation developed for a miniature J-T cooler. It reported that the J-T cooler produces a cooling density that is twice the Integrated circuit chip's heat release density.

Chua[8], *et al.* developed a geometric model for the cryocooler of Hampson-type to develop a better understanding of the tube-and-fin heat exchanger with a double helix. Based on the geometric model, a design tool was developed which provided manufacturers with more realistic and practical design solutions than the commonly used random procedures. Chou and Chien[9], carried out a numerical simulation for the transient characteristics of a miniature J-T cryocooler. The simulation was used in establishing a computer-aided design-based tool. The spatial temperature distributions of hot and cold streams of gas were observed along the heat exchanger during the process of cool-down. Based on the observations, a reduction in size and weight of the currently used J-T cryocooler was proposed.

Chien[10], *et al.* proposed a revised design of a dual-orifice J-T cryocooler. The design was produced based on numerical simulations conducted for transient state operational characteristics of a self-regulating J-T cryocooler. The modified design proposed to effectively stabilize temperature and mass flow rate. Hong[11], *et al.* investigated a miniature J–T cryocooler using a high-pressure reservoir with different initial pressures of nitrogen gas. The cool-down characteristics of the cooler were studied. The effect of supply pressure and cold tip temperature on the mass flow rate was also studied. Hong[12], *et al.* predicted the thermodynamic behavior of the J-T cryocooler heat exchanger utilising nitrogen and argon gases. The decrease in heat exchanger effectiveness was observed when the mass flow rate was increased. However, with an increase in pressure, the corresponding reduction in ideal cooling capacity was not observed.

Aboubakri[13], *et al.* numerically and experimentally investigated the effects of needle clearance and supply pressure on single-phase compressible gas flow in a restricted micro-orifice which provides inputs for the design of a miniature J–T cryocooler. Geng[14], *et al.* designed a throttling and heat exchange structure for simultaneous heat transfer and distributed JT (DJT) effect. A printed circuit heat exchanger (PCHE) was utilized for fabricating a distributed J-T cooler with pillars and thermal performance parameters such as cooler power, cold-end temperature, cooling power, and temperature distribution were tested with argon and nitrogen as refrigerants. Chen[15], *et al.* numerically investigated forced convection in the case of helically coiled mini-tubes for the high-pressure argon at low-temperature. Also, temperature distribution and velocity on the helical coil cross-section and local Nusselt number variation

along the coil length and its periphery are discussed. Chen[16], *et al.* proposed a non-isometric helically coiled heat exchanger with a first-dense-then-sparse type structure for improving the performance of Joule-Thomson (JT) cryocoolers.

Cao[17], *et al.* developed a numerical model for investigating the clogging dynamics in a JT micro cooler operating with nitrogen gas. The model assessed the temperature profile, and water molecule deposition rate of water molecules along the counter-flow heat exchanger and the orifice end of the cooler operating with nitrogen gas. In J-T cooling systems, ejectors are used for the creation of sub-atmospheric pressures and to recover expansion work, thereby achieving lower temperatures and better system efficiencies. Geng[18], *et al.* developed a 1-D ejector model, a 1-D finite-element model of CFHXs, and a cryocooler model for optimizing ejector-equipped JT cryocoolers. Yunwei[19], *et al.* analysed the steady working states of a J-T cryocooler with different typical high pressures to predict changes in the cooling capacity characteristics of a JT cryocooler enabling energy saving and optimal space usage primarily for space applications.

1.1 Motivation for the Present Work

Compact recuperative heat exchangers with high efficiencies are part of critical technologies required necessary cooling for various industrial applications as well as in defense application scenarios. The latter application entails employing these heat exchangers in their miniaturized form, which are quite sensitive to several geometrical influences, process design, cooling gas utilised and clogging dynamics. The predictability of on-board operation of these heat exchangers significantly influences the performance of various projectile systems that may perform time critical missions both in offensive as well as defensive roles. Several studies separately evaluating theoretical, numerical, and experimental performance for various geometries have been reported. However, very limited data is available for a comprehensive study targeting all these aspects for a given heat exchanger geometry providing significantly better insight into mechanics of heat exchanger operation.

The present investigation attempts a comprehensive approach to develop and predict recuperative H-E's performance for J-T cooler by amalgamating the geometry generation utilizing the effectiveness-NTU theoretical approach and subsequently putting forth a numerical approach for its thermo-physics analysis. The approach is novel as this not only enables refining the heat exchanger's geometry but also predicts temperature profiles along H-E facilitating parametric studies on diverse influencing parameters.

The validation studies for a typical case of argon gas against commercial software results have also been carried out to examine the thermo-physics model. Further, a comparative analysis of the modeling and experimental results has also been presented, which is quite imperative to ascertain the efficacy of the thermos-physics model.

2. DESCRIPTION OF MINIATURE JT COOLER

A typical miniature J-T cryocooler is shown in Fig. 1 and its T-s diagram is shown in Fig. 2. The recuperative type heat exchanger of the J-T cryocooler consists of a capillary tube, which is helically wound around a cylindrical mandrel. In order to increase the heat transfer rate of the shell side, the capillary tube is finned in the radial direction. The sum of the fin thickness and the gap between two fins is called the fin pitch. The helical capillary together with the mandrel is placed inside a cylindrical shield. The mandrel and shield form the framework of the cryocooler. The orifice is placed at the end of the heat exchanger. The finned capillary is connected to the orifice. Hot high-pressure (h.p.) stream of gas (1) passes through a heat

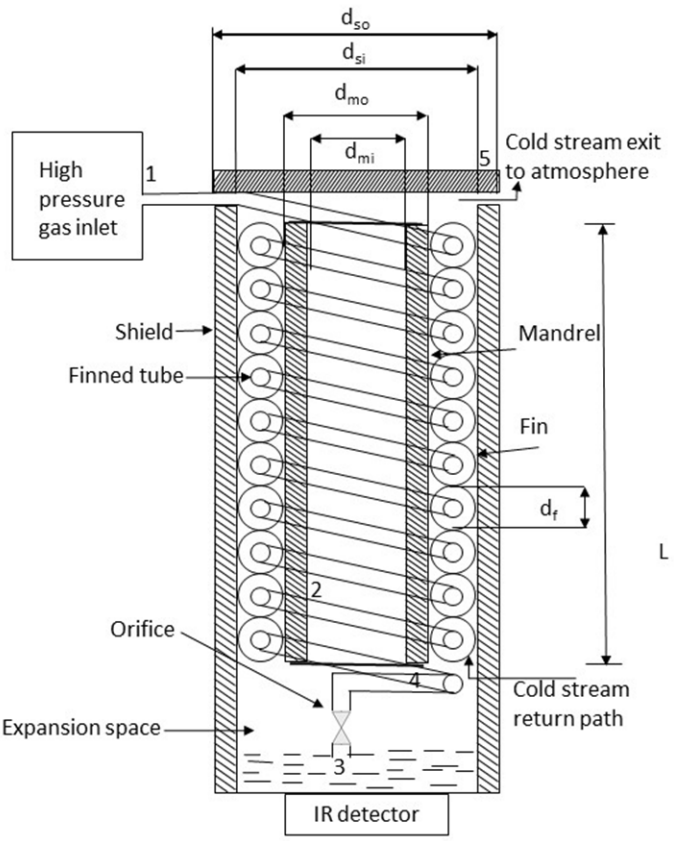

Figure 1. Schematic of a Joule-Thomson cooler, with recuperative counter flow heat exchanger.

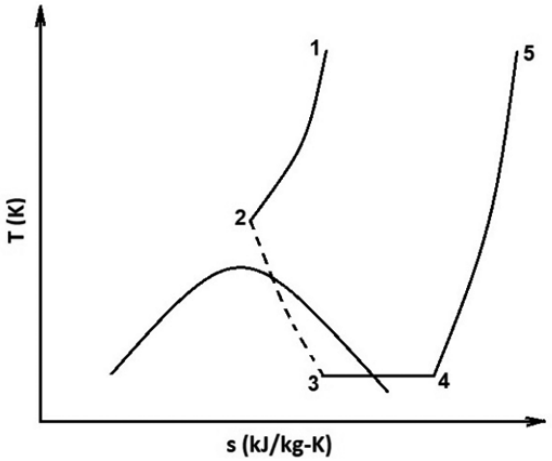

Figure 2. Temperature-entropy diagram for typical operation of J-T cooler employing argon gas.

exchanger. Cold low-pressure (l.p.) stream (4) flows through the space between the outer diameter of the mandrel and the inner diameter of the outer shield (shell). The top end of cooler (5) is the heat exchanger's hot end (at ambient temperature), while the bottom end (3,4) is the cold end (typically at 80 K/90 K). The high-pressure (2) gas expands through an orifice into an evaporator (or reservoir) space (at the bottom of the cooler) and is cooled by Joule-Thomson effect. Under a steady state condition, a portion of the gas liquefies after isenthalpic expansion through the orifice. This liquid cryogen extracts heat from the target body to be cooled. The geometrical and thermal properties of the J-T cooler prototype being studied are given in Table 1.

Table 1. Geometric and thermal parameters of JT cooler prototype

Geometric Parameter	**Value**
Capillary Tube inner diameter d_{ci} (mm)	0.303
Capillary Tube outside diameter d_{ci} (mm)	0.46
Mandrel diameter d_{ci} (mm)	8.16
Cooler diameter d_{mo} (mm)	10.3
Helical coil diameter D_h (mm)	9.23
Fin height (mm)	0.305
Fin pitch (mm)	0.242
Fin Thickness (mm)	0.075
Fin density (fins/mm)	4.13
Thermal parameter	**Value**
Overall Heat Transfer Coefficient ($Wm^{-2}\ K^{-1}$)	196.81
Effectiveness	0.977

3. THEORETICAL AND THERMOPHYSICS ANALYSIS

Theoretical analysis for the geometry of the Joule Thomson cooler model is done for specified thermal performance specifically for the cooling capacity of the J-T cooler required. The underlying assumptions for the analysis are as follows:

- J-T Cooler operates under steady state condition
- Gas streams operate at a temperature average of the inlet and outlet temperatures
- Spatial and temporal temperature profile along the longitudinal direction is neglected

Considering the above-stated assumptions, the heat exchanger geometry is developed and analysed. The mathematical formulation concerning the theoretical model of the J-T heat exchanger is discussed in the following section.

3.1 Geometrical Parameters of the J-T Cooler

Wetted area:

$$A_w = \left[\frac{\pi}{4}\times\left(d_{of}^2 - d_{ofb}^2\right)\times 2 + \pi\times d_{ofb}\times g_f\right]\times N_f \quad (1)$$

Free volume:

$$\frac{\pi}{4}\times\left(d_{of}^2 - d_{ofb}^2\right)\times g_f \times N_f \quad (2)$$

Equivalent diameter:

$$D_e = \frac{\left(4\times Free\ Volume\right)}{A_w} \quad (3)$$

3.2 Thermo-Fluidic Parameters of the J-T cooler

Cooling capacity:

$$Q_{cool} = \dot{m}\left(H_4 - H_3\right) \quad (4)$$

Overall heat transfer coefficient:

$$\frac{1}{U} = \left[\frac{1}{\left(\eta_f\times h_c\right)}\right] + \left[\frac{\frac{A_{o,c}}{A_{o,h}}}{\eta_{o,h}\times h_h}\right] + \left[\frac{A_{oc}\ln\left(\frac{d_{of}}{d_{if}}\right)}{2\pi kL}\right] \quad (5)$$

wherein, correlations for the heat transfer coefficient are given by Flynn[20].

Convective heat transfer coefficient:

$$h = \frac{kNu}{D_e} \quad (6a)$$

Hot stream:

$$h_h = 0.023 C_{p_h} G_h\ \mathrm{Re}_h^{-0.2}\ \mathrm{Pr}_h^{-2/3}\left(1+3.5\frac{D_e}{D_h}\right) \quad (6b)$$

where, $G_h = m/A_h$ $D_e = d_{ci}$ (inside diameter of the capillary tube) and D_h =Helix diameter

Cold stream:

$$h_c = 0.236 Cp_c G_c\ \mathrm{Re}_c^{-0.4}\ \mathrm{Pr}_c^{-2/3} \text{ where, } G_c = \dot{m}/A_c \quad (6c)$$

Reynolds number: $Re = \frac{D_e G}{\mu}$ (6d)

The ectiveness is calculated using standard principles using No. of transfer Units (NTU) as given by Holman[21] & Hong[11], *et al*.

Effectiveness: $\varepsilon = \frac{1-e^{(-NTU(1-C_r))}}{1-C_r e^{(-NTU(1-C_r))}}$ (7)

wherein,

No. of transfer units: $NTU = \frac{UA}{C_{\min}}$ (7a)

Ideal effectiveness: $\varepsilon = \frac{T_{c,o}-T_{c,i}}{T_{h,i}-T_{c,i}}$ (7b)

Pressure drop: $\Delta P = f\left(\frac{L}{D}\right)\rho\frac{V^2}{2}$ (8)

Also, the fanning friction factors for hot and cold streams are given by Flynn[20] as follows:

$$f_h = 0.184 Re_h^{-0.2}\left(1+3.5\frac{D_e}{D_h}\right) \quad (8a)$$

$$f_c = 2 Re_c^{-0.15}\left(0.088 + 0.16\frac{X_L}{\left(X_T-1\right)^{-n}}\right) \quad (8b)$$

Here, $X_T = p_T/d_{of} = D_h/d_{of}$ $X_L = p_L/d_{of}$ where, p_T and p_L are transverse and longitudinal pitch respectively, and

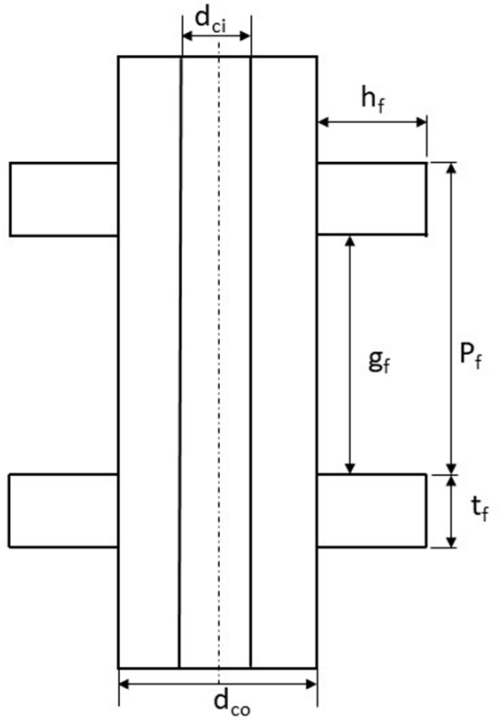

Figure 3. Geometry of helical tube fin.

$n = 0.43 + {}^{1.13}\!/_{X_L}$ corresponding to the fin geometry shown in Fig. 3.

Further, the liquid fraction in the evaporator may be determined considering typical heat exchanger efficiency using the relation as follows:

$$x = \frac{H_4 - H_3}{H_4 - H_f} \tag{9}$$

It is worth noting here that the mass flow rate of active gas undergoing isenthalpic expansion is controlled by the backpressure and orifice throat area. Typical relation for determining mass flow rate for a choked condition for a given fixed area orifice and known backpressure and stagnation temperature conditions suggested by James[22] is given as:

$$\dot{m} = \frac{p_o A}{\sqrt{T_o}} \sqrt{\frac{\gamma}{R}} \left\{ \frac{2}{\gamma + 1} \right\}^{\frac{\gamma+1}{2(\gamma-1)}} \tag{10}$$

where, the discharge coefficient (ratio of actual or measured flow rate to theoretical flow rate) is taken as unity. In this context, Hong[11-12], *et al.* have treated mass flow as a variable independent of pressure. Maytal[23], *et al.* have treated free mass flow and recuperative mass flow separately, having direct and square root proportionality respectively. However, in the present study, the mass flow computations are strictly based on Eq. (10), considering a fixed area orifice operating under choked flow conditions.

Although the theoretical analysis discussed is vital for developing the J-T heat exchanger geometry but has obvious limitations in the prediction of an accurate temperature profile in the exchanger in presence of a mandrel or shield. Furthermore, the theoretical models also have potential shortcomings emanating from the underlying assumptions made. Therefore, comprehensive numerical modeling is performed and thermal analysis is conducted on the developed J-T cooler geometry.

Note that the present rigorous numerical analysis essentially involves generating the temperature profiles along the viz., h.p. gas flow, the wall separating the h.p. and the l.p. gas flows, l.p. gas flow, mandrel, and shield. In addition, the material properties of the shield, boundary wall, and mandrel, along with pressure and temperature dependences of gas (both in h.p. and the l.p. streams), are accounted for in the present numerical modeling using heat flux balancing methodology outlined by Anderson[24], *et al.* & Singhal[25], *et al.* is given as:

Hot stream: $$\dot{m}_h C_{ph} \frac{dT_h}{dx} = h_h p_{ci} \left(T_w - T_h \right) \tag{11}$$

Cold stream:

$$\dot{m}_c C_{pc} \frac{dT_c}{dx} = h_h \left[p_{co} \left(T_c - T_w \right) + p_{si} \left(T_c - T_s \right) + p_{mo} \left(T_c - T_m \right) \right] \tag{12}$$

Wall temperature:

$$k_w A_w \frac{d^2 T_w}{dx^2} = h_h p_{ci} \left(T_w - T_h \right) + h_c p_{co} \left(T_w - T_c \right) \tag{13}$$

Mandrel temperature:

$$k_m A_m \frac{d^2 T_m}{dx^2} = h_c p_{mo} \left(T_m - T_c \right) \tag{14}$$

Shield temperature:

$$k_s A_s \frac{d^2 T_s}{dx^2} = h_c p_{si} \left(T_s - T_c \right) + h_r p_{so} \left(T_s^4 - T_{amb}^4 \right) \tag{15}$$

Here, the radiation heat transfer coefficient h_r (in Eq.15) is given as:

$$h_r = \frac{\sigma}{\frac{1}{\varepsilon_s} + \frac{A_{so}}{A_r} \left\{ \frac{1}{\varepsilon_r} - 1 \right\}} \tag{16}$$

The J-T cooler numerical model in the present case is tested for Argon gas but may be easily configured for various possible combinations of gases and the tube, shield, and mandrel materials to arrive at the most optimum design solution.

Here, the radiation term is linearized by using the equation as suggested by Patankar[26] viz. $S = S_c + S_p T_p$. It may be made a known source term instead of making it temperature-dependent by considering S_p=0 and $S_c = \alpha \left(T_{amb}^4 - T^{*4} \right)$. T^* in the expression is the cell temperature of the previous iteration (assumed value at initialization), and it is known.

Further, the pressure drop being another significant parameter in the design of the J-T heat exchanger's length, the pressure variation along the flow direction may be computed employing the following relation.

$$\frac{dp}{dx} = \frac{\frac{2f}{\rho D_h}}{\frac{d\rho}{p^2 dp} - \frac{1}{G^2}} \tag{17}$$

In governing equations, a set of variables are suitably non-dimensionalized. All the temperature terms are normalized with $(T_1\text{-}T_4)$. X –coordinate is normalized with L. All areas are normalized with $A_c = \Sigma(A_{co}, A_{mo}, A_{si})$. Similarly, the wall thermal resistance is normalized with mC_{pc} (happens to be C_{min}).

An additional approximation of neglecting variation of thermo-physical gas properties with temperature is made while

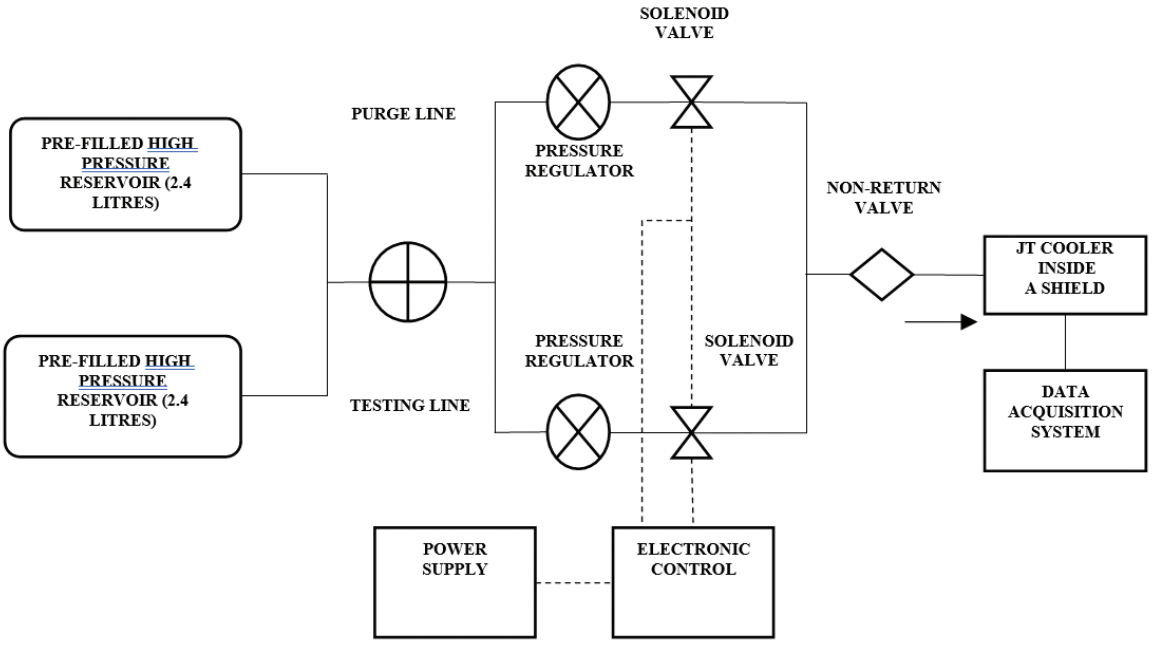

Figure 4. Schematic of experimental test setup.

Table 2. Contamination levels accepted for pure gases used for detector cooling applications

Constituents / contaminants	Units	Limits (Defence Standard 58/96)
Water vapour	ppm	≤ 1.0 ppm
CO2	ppm	≤ 0.6
Methane	ppm	≤ 9.0
Other Hydrocarbons (Total)	ppm	≤ 0.05
Particulate matter	µm	≤ 5

Cold end (x=L): $T_c = T_{cin}$ & $\frac{dT_w}{dx} = \frac{dT_m}{dx} = \frac{dT_s}{dx} = 0$

4. EXPERIMENTAL TEST SETUP & PROCESS STEPS

The testing involves the passing of high-pressure Argon through a helically wound finned tube over the mandrel in an integrated Joule Thomson cryocooler assembly. High-pressure gas from the finned tube on passing through an orifice produces a JT effect resulting in cooling with gas reaching a two-phase state (vapor-liquid) corresponding to pressure and temperature

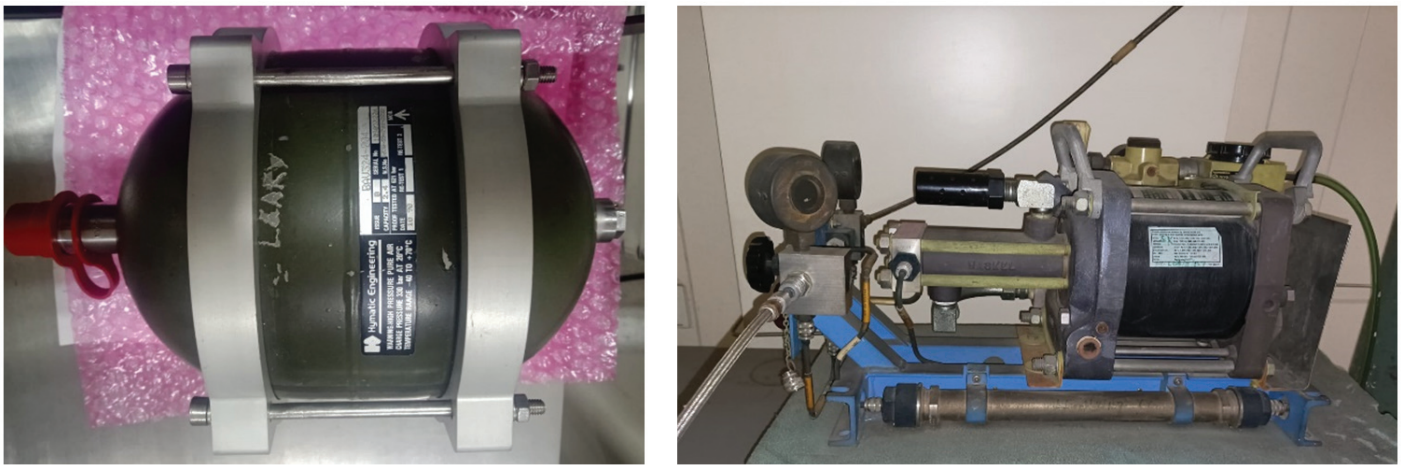

(a) (b)

Figure 5. (a) High pressure vessel and, (b) Gas booster.

solving the above-stated five coupled differential equations (11)-(15). This assumption is essentially valid primarily due to the low-temperature regime of operation of J-T coolers.

As stated below, the Dirichlet boundary conditions are employed at the cold as well as the hot end of the J-T heat exchanger.

Hot end (x=0): $T_h = T_{hin}, T_w = T_{hin}, T_m = T_{hin} = T_s = T_{hin}$

at the exit. The expanded gas on its return flows over the helical tubes where the exchange takes place through the fins present resulting in cooling of entering high enthalpy gas. This heat exchange increases the JT coefficient of pure argon gas during expansion. To validate the results of the simulation, experiments were done on an experimental setup with a layout as shown in Fig. 4. The configuration is as discussed in[27], wherein the

J-T cooler cryo-chamber assembly is interfaced with a high-pressure reservoir in a system having solenoid and regulation valves along with molecular sieve filter and particulate filters.

The major steps in preparation and experimenting are as follows:

4.1 Supply of High Purity Gas

In order to avoid clogging of the JT cooler during its cooling to a cryogenic temperature, the purity of gas used (Argon/ Nitrogen) is of extreme importance. Maximum permissible contamination levels for pure Gases for detector cooling applications as per the Defence Standard 58/96 are listed in Table 2. Nitrogen or Argon gas of 99.9995 % purity is used in the JT cooler.

4.2 Filling up of High-Pressure Vessel

In the experiments, a high-pressure vessel (Make: Hymatic) as shown in Fig.5(a) is used. The vessel has a capacity of 2.4 liters of water volume and may operate at a maximum pressure of 400 bar. These high-pressure vessels are filled by a gas-booster (AG 75: Model: Haskel) as shown in Fig 5(b) having a nominal pressure ratio of 75:1. It is a single-acting, single-stage gas booster that utilizes air pressure for boosting gas pressures up to 310 bar in our case.

4.3 Assembly of High-Pressure Reservoir & System Leak Check

The high-pressure reservoir is attached to the setup through a quick-release valve and all the components, and pipelines assembled in the system are checked for leakage through a dry run before the start of the experiment.

4.4 Purging of System and the JT Cooler

Each time before carrying out the experiment, the complete system, and the JT cooler are separately purged at a very low pressure to ensure the elimination of impurities from the system and the cryocooler. This helps in minimizing the possibility of clogging of cryo-cooler during its operating cycle.

4.5 Actual Experimentation

After completion of purging, the high-pressure reservoir is regulated to a pressure of 210 bar and the experiment is initiated. The reservoir pressure may vary during the experiment, but the system inlet pressure remains the same by employing suitable gas pressure regulation. A solenoid valve is used for switching on/off the gas flow. The gas first passes through a filter assembly before entering the cryocooler. The setup is remotely operated employing a customized data acquisition system (DAS). The temperature measurements are carried out using a suitable Resistance Temperature Device, Pt- 100 or Pt-1000 (PR-17 Model: Omega). When the observed temperature variation inside the JT cooler assembly is within a range of ±1K, is assumed to have reached steady-state operation. Required data of the cooler during operation is collected in this state.

5. RESULTS AND DISCUSSION

Pressure differentials in J-T coolers are large and variations may also exist in flow characteristics of the orifice owing to different geometries such as dimension, shape, profile, and roughness. Hence it is important to verify the orifice flow characteristics, including the overall discharge coefficient, and precisely calibrate the exiting flow rate with backpressure. The effect of the mass flow rate of the gas on the cooling characteristics of the J-T cooler and its effectiveness have been theoretically evaluated and compared with the thermophysical model in MATLAB. Results are plotted in Fig. 6 and Fig. 7 and are in close agreement with variations reported by Hong[11], *et al.*

It may be inferred from Fig. 6 that the J-T cooler's effectiveness is considerably affected by the cooling gas mass flow rate and pressure changes. A significant drop in J-T miniature cooler effectiveness is observed with an increase in the mass flow rate of gas over a range of 10 to 50 MPa. This is primarily because of a decrease in heat exchanger transfer units between heat-exchanging streams. At 10 MPa inlet pressure, the deterioration in effectiveness is substantial compared to cases of other higher gas stream pressure. It is found that in the lower mass flow rate range < 0.2g/s of cooling gas, the effectiveness attains a high value close to 1.0 at all cooling gas stream pressure.

It is noticed that the J-T cooler cooling capacity considerably increases when the cooling gas mass flow rate is

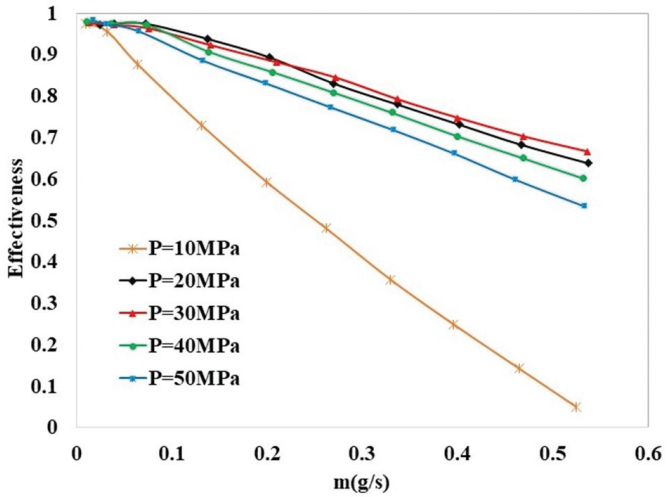

Figure 6. Effectiveness variation with mass flow rate for argon gas .

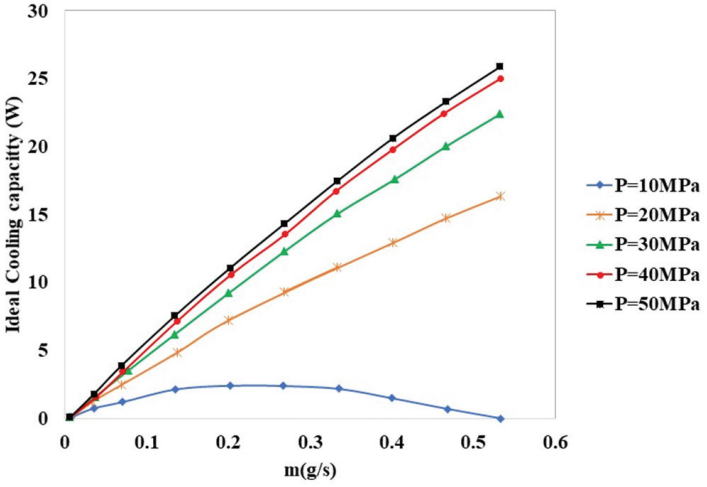

Figure 7. Cooling capacity variation with mass flow rate for argon gas.

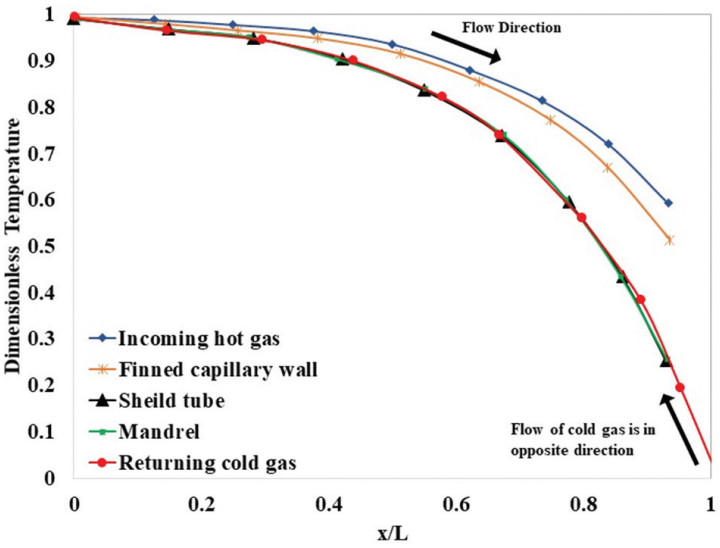

(a)

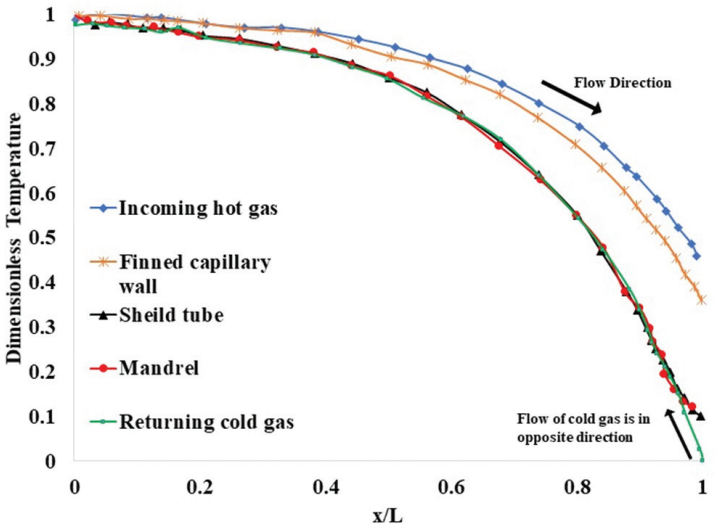

(b)

Figure 8. (a) Predicted temperature profile from COMSOL multiphysics and (b) Predicted temperature profile from MATLAB code.

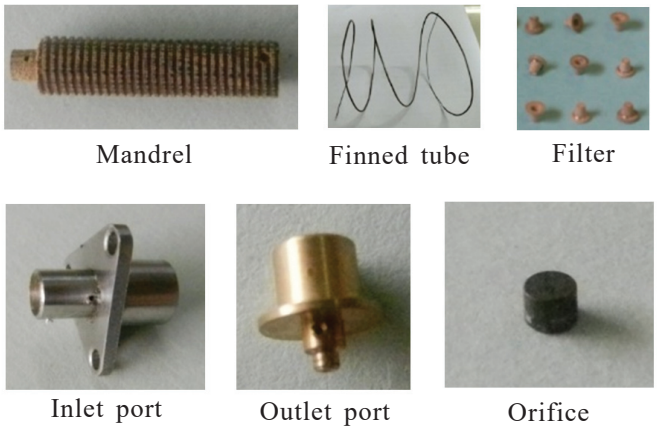

Figure 9. Components of miniature J-T cooler.

increased and the dependence is almost linear except for the low cooling gas stream pressure of 10 MPa (Fig.7). It is also notable that J-T cooler cooling capacity with gas flow rate shows a sharp increase for cooling gas stream pressure higher than 20 MPa. It is worth highlighting in the case of low stream pressure of 10 MPa, the cooling capacity first increases followed by a decrease in flow rate. This is on account of extensive frictional losses limiting the cooling capacity of the gas stream.

The coupled differential equations (11)-(15) have been solved by using Runge- Kutta method in MATLAB. To validate the results, the solution using the standard algorithm in the COMSOL Multiphysics package has also been carried out, invoking the relevant equations of energy transfer. The generated comparative results are shown in Fig. 8(a) and Fig. 8(b).

Here, the temperature profiles for the hot stream, cold stream, wall, mandrel, and shield have been specifically compared. The temperature profiles are in close agreement both qualitatively as well as in terms of normalized magnitude(s). The temperature profile of the cold stream, shield, and mandrel are essentially overlapping. The temperature profiles for the wall and the hot stream are marginally different. The good matching of the J-T cooler results obtained from in-house developed MATLAB code and COMSOL Multiphysics solver confirms the accuracy of the computation.

The numerical studies carried out employing the thermo-physics model enable the prediction of temperature profiles along the H-E elements. However, certain critical aspects such as cool-down time may only be determined experimentally, which will help in ascertaining the suitability of the code

Figure 10. J-T cooler integrated with glass dewar.

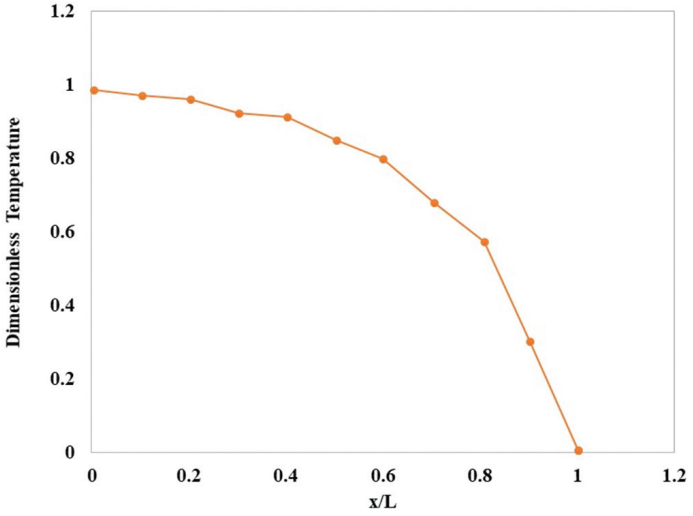

Figure 11. Observed temperature profile along the J-T cooler mandrel.

Table 3. Comparison of experimental data with MATLAB results of $T_{cold,\ out}$

$P_{hot,in}$ (MPa)	$T_{hot,in}$ (K)	$T_{cold,in}$ (K)	$T_{cold,\ out}$ (K)		
			Experiment	COMSOL	Error %
25.855	300.23	88.88	291.50	290.64	0.295
24.132	300.54	89.25	292.08	291.20	0.3013
22.408	301.15	90.05	293.35	294.15	0.273
20.684	300.85	89.42	292.78	291.88	0.3074

Table 4. Comparison of experimental data with COMSOL results of $T_{cold,\ out}$

$P_{hot,in}$ (MPa)	$T_{hot,in}$ (K)	$T_{cold,in}$ (K)	$T_{cold,\ out}$ (K)		
			Experiment	MATLAB	Error %
25.855	300.23	88.88	291.50	290.04	0.5009
24.132	300.54	89.25	292.08	290.65	0.4896
22.408	301.15	90.05	293.35	294.75	0.477
20.684	300.85	89.42	292.78	291.62	0.3962

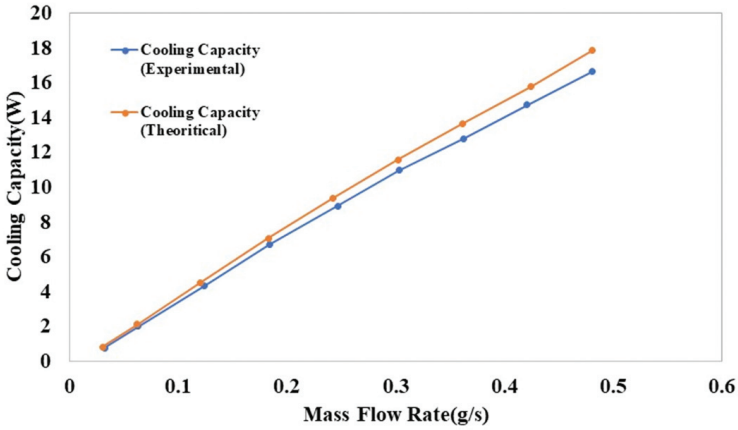

Figure 12. Cooling capacity of J-T cooler with mass flow rate.

Table 5. Comparison of experimental and simulation data of cooling capacity

Mass flowrate (g/s)	Cooling capacity (W) (Experimental)	Cooling capacity (W) (Simulation)	Error (%)
0.030	0.760	0.7955	4.671
0.062	1.998	2.095	4.854
0.120	4.302	4.514	4.928
0.183	6.715	7.055	5.063
0.243	8.902	9.372	5.279
0.302	10.967	11.557	5.379
0.362	12.784	13.643	6.719
0.423	14.733	15.769	7.031
0.480	16.621	17.852	7.406

for practical use. The cool-down performance of JT coolers exhibited during experimentation enables the designer in making design optimisations for the realisation of the initial prototype for the intended objective before commencing production in larger numbers.

To validate the results of a simulation, in-house experiments were carried out utilizing the developed experimental setup discussed already in an earlier section. In Fig 9, realized components of a miniature type of J-T cooler based on a recuperative heat exchanger are shown in Fig. 9 whereas Fig. 10 shows double walled glass dewar with an inserted prototype of a cooler inside it.

The graph in Fig. 11 shows measured temperature variation along the JT cooler mandrel along with the predicted temperature profile. It is clear that the measured temperature profile closely follows the predicted temperature profile employing the thermo-physics model. The mandrel temperature gradually reduces as x/L as increases from 0 to 1. It is observable that the reduction in temperature along the mandrel is not essentially linear.

Since the model employs specific equations applicable to the energy balance of the problem, the main advantage is that the temperature predicted is precise and is much less time-intensive. Experiments were carried out with four regulated inlet pressure of Argon and the experimental values of temperature of the cold stream of gas ($T_{cold,\ out}$) were compared with those predicted by MATLAB and COMSOL Multiphysics. The comparison is tabulated in Tables 3 and 4. It is observed that absolute prediction error relative to the measured value is within 0.3 % and 0.5 % for MATLAB and COMSOL Multiphysics respectively.

Further, the effect of variation of the cooling capacity of the J-T cooler with cooling gas mass flow rate was also studied experimentally and the observed trends are plotted in Fig. 12 against the theoretically predicted variation.

The theoretical predictions are commensurate with the experimental observations. It is clear that on increasing the mass flow rate of the cooling gas, a considerable rise in the J-T cooler's cooling capacity is produced. Moreover, the increase in cooling capacity with mass flow rate is nearly linear. The percentage error calculated between theoretical and experimental values at a higher mass flow rate is close to 7 %. Table 5 tabulates the experimental results and comparison between the theoretical and experimental values of cooling capacity.

Further, the effect of variation in mass flow rate owing to change in orifice diameter in terms of its cool downtime (Time for reaching target temperature i.e., 88 K) was experimentally studied.

Figure 13 depicts the variation of the cool-down time (CDT) with J-T cooler orifice diameter. Two orifices of diameter 75 µm and 100 µm fabricated using a high-speed drilling process were integrated with the outlet port of the JT cooler. It is noticed that for higher orifice diameters, the cool-down time is greatly reduced. The flow rate for a given supply pressure is a strong function of orifice diameter and increases by nearly 30 % from 75 µm orifice to 100 µm orifices. Hence, the targeted temperature of 88K is reached much faster for the

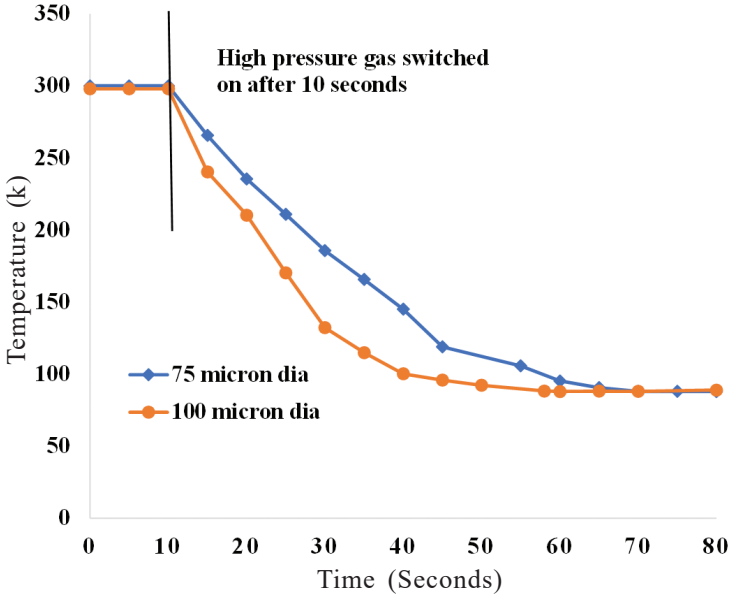

Figure 13. Effect of variation in J-T cooler orifice on cool down time.

JT cooler with 75 µm orifice in ~48s against the JT cooler with 100 µm orifice which took almost 65s to reach 88 K.

6. CONCLUSION

Detailed theoretical analysis and thermo-physics modeling of the thermal performance of a miniature J-T cooler together with a recuperative H-E under steady-state conditions have been carried out. The recuperative heat exchanger has been theoretically assessed employing the effectiveness-NTU method predicting the effectiveness as ~97%. The experimentally observed J-T cooler cooling capacity compares well with the theoretical predictions showing a maximum variation of ~7%. Further, detailed thermo-physics modeling of the H-E is also reported predicting the temperature profile along the gas stream, mandrel, and shield for typical operating conditions. MATLAB has been used for developing the code for the same and the solution is obtained using the Runge-Kutta method. Validation of the results has been done employing COMSOL multi-physics and they are observed to be in close agreement. The benefit lies in the code being significantly less time and computational resource intensive. The results have been experimentally verified and are in close agreement, thereby proving the efficacy of the model developed.

REFERENCES

1. Hu,M.; Zhai,G.; Li,Duo; Fan,Y.; Duan,H.; Zhu,W.& Yang, X. Combination of near infrared and thermal imaging techniques for the remote and simultaneous measurements of breathing and heart rates under sleep situation, *PLOS ONE*, 2018, **13**(1). doi: 10.1371/journal.pone.0190466.
2. Vollmer, M. & Mollmann, K.P. Infrared thermal imaging: fundamentals, research and applications, John Wiley and Sons, 2017.
3. Bhan, R.K. & Dhar, V. Recent infrared technologies, application, trends and development of HgCdTe based cooled infrared focal plane arrays and their characterization, *Opto-Electronics Rev.*, 2019, **27**, 174-193. doi: 10.1016/j.opelre.2019.04.004.
4. Geng, H.; Cui, X.Y.; Weng, J.H.; She, H.L. & Wang, W.Q. Review of experimental research on Joule-Thomson cryogenic refrigeration system, *Appl. Therm. Eng*., 2019, **157**, 113640. doi: 10.1016/j.applthermaleng.2019.04.050.
5. Maytal, B.Z. & Pfotenhauer, J.M. Miniature Joule-Thomson cryocooling: Principles and practice[M]. Springer Sci. Business, 2012. ISBN: 978-1-4419-8285-8.
6. Xue, H.; Ng, N.G. & Wang, J.B. Performance evaluation of the recuperative heat exchanger in a miniature Joule-Thomson cooler, *Appl. Therm. Eng*., 2001, **21**, 1829-1844. doi: 10.1016/S1359-4311(01)00050-3.
7. Ng, K.C.; Xue, H. & Wang, J.B. Experimental and numerical study on a miniature Joule-Thomson cooler for steady state characteristics, *Int. J. Heat Mass Transfer*, 2002, **45**, 609-618. doi: 10.1016/S0017-9310(01)00165-X.
8. Chua, H.T.; Wang, X.L. & Teo, H.Y. A numerical study of the Hampson- type miniature Joule-Thomson cryocooler, *Int. J. Heat Mass Transfer*, 2006, **49**, 582-593. doi: 10.1016/j.ijheatmasstransfer.2005.08.024.
9. Chou, F.C.; Pai, C.F.; Chien, S.B. & Chen, J.S. Preliminary experimental and numerical study of transient characteristics for a Joule- Thomson cryocooler. *Cryogenics*, 1995, **35**, 311-316. doi: 10.1016/0011-2275(95)95349-J.
10. Chien, S.B.; Chen, L.T. & Chou, F.C. A study on the transient characteristics of a self-regulating Joule Thomson cryocooler. *Cryogenics*, 1996, **36**, 979-984. doi: 10.1016/S0011-2275(96)00085-9.
11. Hong Y., Park S.J. & Choi, Y.D. A numerical study of the performance of a heat exchanger for a miniature Joule-Thomson refrigerator. *In* Int. Cryocooler Conference Cryocoolers, 2009, **15**, 379-386. doi: 10.1063/1.3422265.
12. Hong,Y.J.; Park,S.J.; Kim, H.B. & Choi, Y.D. The cool-down characteristics of a miniature Joule-Thomson refrigerator. *Cryogenics*, 2006, **46**, 391-395. doi: 10.1016/j.cryogenics.2005.07.008.
13. Aboubakri, A.; Sadaghiani,K.A.; Akgonul, S.; Erdogmus, B.A.; Baki, M.; Can, F.; Sabanovic, A. & Kosar, A. Numerical and experimental investigation of the effect of micro restriction geometry on gas flows through a micro orifice. *Fluids,* 2022, **7**, 151. doi: 10.3390/fluids7050151.
14. Geng, H.; Cui1, X.; Hailong, S. & Zhihao. Characterization of a distributed Joule-Thomson effect cooler with pillars, *Int J. Energy Res.*, 2021, 1–13. doi: 10.1002/er.6756.
15. Chen, L.; Caic, J.; Lvb,K.; Yangb, X.; Chena, S.; & Houa, Y. Distributed Joule-Thomson effects and convective heat transfer of high-pressure argon gas flow in helically coiled mini-tubes. *Appl. Thermal Eng.*, 2020, 181, 115955. doi: 10.1016/j.applthermaleng.2020.115955.

16. Chen, H.; Liu, Q-s.; Liu, Y-w. & Gao, B. Optimal design of a novel non-isometric helically coiled recuperator for Joule–Thomson cryocoolers. *Appl. Thermal Eng.*, 2019. doi: 10.1016/j.applthermaleng.2019.114763.
17. Cao, H.S.; Vanapalli, S.; Holland, H.J.; Vermeer, C.H. & Brake, H.J.M ter. Numerical analysis of clogging dynamics in micromachined Joule-Thomson coolers. *Int. J. Refrig.*, 2017. doi: 10.1016/j.ijrefrig.2017.05.023.
18. Geng, L.H.; Cao, H.S.; Li, J.M. & Jiang, P.X. Design and performance analysis of an ejector-equipped Joule–Thomson cryocooler. *Appl. Thermal Eng.,* 2021, **190**, 116779. doi: 10.1016/j.applthermaleng.2021.116779.
19. Yunwei, S.; Dongli, L.; Sifan, C.; Qinyu, Z.; Lei, L.; Zhihua, G. & Min, Q. Study on cooling capacity characteristics of an open-cycle Joule-Thomson cryocooler working at liquid helium temperature. *Appl. Thermal Eng.,* 2019. doi: 10.1016/j.applthermaleng.2019.114667.
20. Flynn, T.M. Cryogenic engineering, Marcel Dekker New York USA, 1997. doi: 10.1002/vipr.19980100419.
21. Holman, J.P. Heat and mass transfer, Tata McGraw Hill, 8th edition, 1989.
22. John, James E.A. Gas dynamics, 2nd edition, Pearson Prentice Hall, 2009.
23. Maytal, B.Z. Open cycle Joule-Thomson Cryocooling by mixed coolant. *In* International cryocooler conference, cryocooler 16, 2011.
24. Anderson, D.A.; Tannehill, J.C. & Pletcher, R.H. Computational Fluid Mechanics and Heat Transfer CRC Press, 3rd Edition, 2012. doi: 10.1201/b12884
25. Singhal, M.; Gaurav Singhal, G.; Verma, A.C.; Sushil Kumar, S. & Manmohan Singh, M. Numerical investigation of steady sate thermal behavior of an infrared detector cryochamber. *Thermal Sci.*, 2017, **21**(3), 1203. doi: 10.2298/TSCI140617107S
26. Patankar, S.V. Numerical heat transfer, hemisphere publishing corporation, 1980.
27. Singhal, M.; Singhal, G.; Verma, A.C.; Kumar, S. & Singh M. Thermophysics modelling of an infrared detector cryochamber for transient operational scenario. *Infrared Physics Technol.*, 2016, **76**, 103-110. doi: 10.1016/j.infrared.2016.01.023.

ACKNOWLEDGMENTS

The authors thank the Director, of Solid State Physics Laboratory, Delhi, India, for permitting them to carry out the experimental investigations presented in this paper.

CONTRIBUTORS

Mr Mayank Singhal obtained his ME (Thermal Engineering) from Delhi College of Engineering, Delhi. He is working at DRDO. His research interests include hermetic sealing and development of packages of electronic devices and their thermal management.
In the current study, he has conceptualised and initiated the study, created experimental setup and carried out detailed experimental evaluation and validation of results.

Dr Rajesh Kumar obtained his PhD from Jamia Millia Islamia University, Delhi. He is a Professor in Dept. of Mechanical engineering at Delhi Technological University (DTU), Delhi. His current research is in the area of thermal Engineering and Refrigeration and air conditioning.
In the current study, he has contributed in the design of experiments, guided the work and reviewed the manuscript.

Dr R.S. Walia obtained his PhD from IIT, Roorkee. He is currently a Professor in Dept. of Mechanical engineering at Punjab Engineering College, Chandigarh. His major research is in the area of Advanced manufacturing processes.
In the current study, he has contributed in the analysis of the experimental results and finalization of the manuscript.

Dr S.K. Pandey obtained his PhD from IIT, Delhi. Currently he is working at DRDO-Aeronautics Research and Development Board. His areas of research include development and characterisation of semiconductor and ceramic materials.
In the current study, he has guided and given critical inputs for literature survey and experimental setup.